Ferromagnetism in $[Mn(Cp^*)_2]^+$-Derived Complexes: the "Miraculous" Stacking in $[Mn(Cp^*)_2][Ni(dmit)_2]$

Christophe Faulmann,*[a] Eric Rivière,[b] Stéphane Dorbes,[a] François Senocq,[c] Eugenio Coronado,[d] and Patrick Cassoux[a]

Dedicated to Patrick Cassoux on the occasion of his recent retirement[‡]

Keywords: Metallocenes / Magnetic properties / Manganese / S ligands

The synthesis and characterisation (X-ray structure and magnetism) of metal complexes (Ni, Au) with the $[Mn(Cp^*)_2]^+$ cation and the $dmit^{2-}$ and $dmid^{2-}$ ligands are reported. $[Mn(Cp^*)_2][Ni(dmit)_2]$ (**1**) and $[Mn(Cp^*)_2][Au(dmit)_2]$ (**2**) exhibit the same structural arrangement, built on stacks of $[Ni(dmit)_2]^-$ pairs separated by two $[Mn(Cp^*)_2]^+$ cations, showing a $\cdots D^+D^+A^-A^-D^+D^+A^-A^-\cdots$ motif. On the contrary, the $dmid^{2-}$ derivative $[Mn(Cp^*)_2][Ni(dmid)_2]\cdot CH_3CN$ (**3**) exhibits a totally different structure, built on mixed layers composed of one $[Ni(dmid)_2]^-$ unit separated by two $[Mn(Cp^*)_2]^+$ cations, showing a $\cdots D^+D^+A^-D^+D^+A^-\cdots$motif. The layers are separated from each other by perpendicular $[Ni(dmid)_2]^-$ units and solvent molecules. Compound **2** exhibits antiferromagnetic interactions, whereas **1** and **3** exhibit ferromagnetic interactions at low temperature. Moreover, as confirmed by AC and DC magnetic susceptibility measurements, **1** is a ferrimagnet, the first ever derived from a 1,2-bis-dithiolene ligand. The ferromagnetic interactions in **1** and **3** are explained using the McConnell I mechanism.

Introduction

Since the discovery of metamagnetism in the molecule-based solid, $[Fe(Cp^*)_2](TCNQ)$,[1] (Cp^* = pentamethylcyclopentadienyl; TCNQ = tetracyanoquinodimethane), several studies have been carried out with the aim of substituting planar metal-organic complexes with the organic TCNQ acceptor and varying the nature of the metallocene; the complexes $[Fe(Cp^*)_2](TCNE)$[2] (TCNE = tetracyanoethylene), $[Mn(Cp^*)_2](TCNQ)$[3] and $[Mn(Cp^*)_2](TCNE)$[4] have been proven to be bulk ferromagnets. These compounds are structurally analogous, and their structures consist of parallel chains of alternating donor cations (D^+) and acceptor anions (A^-), thus showing a $D^+A^-D^+A^-$ motif.

There are two possible models that may explain the ferromagnetic coupling between the metallocenium $[M(Cp^*)_2]^+$ cation and the acceptor ($TCNE^-$ or $TCNQ^-$) (see ref.[5] and papers cited therein). The first explanation was proposed by Miller et al.[2] and is based on the McConnell II mechanism[6] which involves charge transfer, whereas the second one (based on the McConnell I mechanism[7]) was proposed later by Kahn and co-workers[8] and involves spin polarisation effects. Schweizer and co-workers recently[5] showed that the McConnell I mechanism can partly explain the ferromagnetic interactions within $[Fe(Cp^*)_2](TCNE)$, however no clear-cut evidence for the first or the second mechanism has really emerged. Even more recently, the results of a solid-state NMR study on various paramagnetic metallocenium ions[9] were in agreement with all the requirements for the McConnell I mechanism. Whatever the mechanism, a 1-D structure with a $D^+A^-D^+A^-$ motif was believed to be a prerequisite for the synthesis of molecular ferromagnets.[10] The metal bis-dithiolene complexes $[M(S_2C_2R_2)_2]^-$ have been used as acceptors in order to achieve such 1D-chains, since they are able to form either alternating or segregated stacks, depending on the associated cations. These metal complexes are excellent candidates for achieving the requirements for cooperative magnetic phenomena, due to the presence of peripheral het-

[‡] For his enormous contribution in the field of the $M(dmit)_2$ systems.

[a] Equipe Précurseurs Moléculaires et Matériaux, LCC-CNRS, 205 route de Narbonne 31077 Toulouse Cedex 04, France
Fax: (internat.) +33-5/61 55 30 03
E-mail: faulmann@lcc-toulouse.fr
[b] Laboratoire de Chimie Inorganique, ICMO Bât. 420, Université Paris-Sud, 91405 Orsay Cedex, France.
[c] CIRIMAT ENSIACET, 118, Route de Narbonne, 31077 Toulouse Cedex 04, France
[d] Instituto de Ciencia Molecular (ICMol), Universitat de Valencia, Dr Moliner, 50, 46100 Burjassot, Spain

Supporting information for this article is available on the WWW under http://www.eurjoc.org or from the author.

  DOI: 10.1002/ejic.200300087

eroatoms which might favour extended magnetic interactions. Most of the molecular charge-transfer salts previously synthesised and studied are based on the decamethylferrocenium cation, $[Fe(Cp^*)_2]^+$, in combination with metal bis-dithiolene complexes including those involving the $dmit^{2-}$ ligand[11–14] ($dmit^{2-}$ = $C_3S_5^{2-}$= 2-thioxo-1,3-dithiole-4,5-dithiolato), the mnt^{2-} ligand[15,16] [mnt^{2-} = $(NC)_2C_2S_2^{2-}$ = maleonitriledithiolato] and the tfd^{2-} ligand[15,17] [tfd^{2-} = $(F_3C)_2C_2S_2^{2-}$ = bis(trifluoromethyl)-ethylenedithiolato]. Recent studies have also focused on complexes of edt^{2-} and $dmid^{2-}$ (also called $dmio^{2-}$)[14,18–20] (edt^{2-} = $C_2H_2S_2^{2-}$ = ethylenedithiolato; $dmid^{2-}$ = $C_3OS_4^{2-}$= 2-oxo-1,3-dithiole-4,5-dithiolato).

From the studies on all these complexes, two conclusions can be drawn: their structures do not always exhibit a $D^+A^-D^+A^-$ motif (which is, a priori**,** considered as a disadvantage for producing ferromagnetic molecular compounds), and very few of them exhibit ferromagnetic interactions. Nevertheless, substituting Mn for Fe in the metallocenium part has led to complexes with interesting magnetic properties: $[Mn(Cp^*)_2][Ni(tfd)_2]$,[21] $[Mn(Cp^*)_2][Ni(bdt)_2]$[18] (bdt^{2-} = $C_6H_4S_2^{2-}$ = 1,2-benzenedithiolato) and $[Mn(Cp^*)_2][Ni(dmit)_2]$[22] (**1**) exhibit long range magnetic ordering at low temperature, whereas the $[Fe(Cp^*)_2]$-based analogues only exhibit ferromagnetic interactions. Therefore, with the intention of understanding the differences in the magnetic behaviour, and after the promising results obtained for $[Mn(Cp^*)_2][Ni(dmit)_2]$,[22] we here present a more detailed characterisation of the latter compound and the synthesis and characterisation of two new compounds based on the manganocenium cation, namely $[Mn(Cp^*)_2][Au(dmit)_2]$ (**2**) and $[Mn(Cp^*)_2][Ni(dmid)_2]\cdot CH_3CN$ (**3**).

Results and Discussion

Synthesis

Complexes **1**, **2** and **3** were obtained by slow addition of an acetonitrile solution of $[Mn(Cp^*)_2]PF_6$ [23] in slight excess to an acetonitrile or acetone solution of the appropriate $(nBu_4N)[M(ligand)_2]$ (ligand = $dmit^{2-}$, $dmid^{2-}$) complex. After concentration, a brown microcrystalline powder was collected by filtration, washed several times with acetonitrile and dried in vacuo. Recrystallisation of this powder from various solvents failed and resulted in the same brown powder. In the case of **1**, small single crystals suitable for an X-ray analysis were sometimes isolated from the microcrystalline powder. On the contrary, a large number of single crystals of **2** and **3** suitable for X-ray analyses could be easily isolated from the corresponding microcrystalline powders.

X-ray Structure of 1, 2 and 3

Although the size of the crystals of **1** was very small (0.1 × 0.1 × 0.03 mm^3), an X-ray study was undertaken and resulted in the collection of 15817 reflections, for which only 596 were observed above $2\sigma(I)$. Nevertheless, in spite of this low quality data set, we have been able to solve the structure of **1** without great difficulty. The crystal and experimental data for **1**, **2**, and **3** are summarised in Table 1.

Complexes **1** and **2** are isostructural with $[Fe(Cp^*)_2]$-$[Ni(dmit)_2]$.[11] The asymmetric unit of **1** and **2** contains one $[Mn(Cp^*)_2]^+$ cation and one $[M(dmit)_2]^-$ anion (M = Ni, Au; Figure 1).

The overall structural arrangement consists of $\cdots D^+D^+A^-A^-D^+D^+A^-A^-\cdots$ stacks comprising side-by-

Table 1. Crystallographic data for complexes **1**, **2** and **3**

	$(Cp^*_2Mn)[Ni(dmit)_2]$ (**1**)	$(Cp^*_2Mn)[Au(dmit)_2]$ (**2**)	$(Cp^*_2Mn)[Ni(dmid)_2]\cdot CH_3CN$ (**3**)
Empirical formula	$C_{26}H_{30}MnNiS_{10}$	$C_{26}H_{30}AuMnS_{10}$	$C_{28}H_{33}MnNNiO_2S_8$
M	776.75	915.01	785.68
Crystal system, space group	Triclinic, $P\bar{1}$	Triclinic, $P\bar{1}$	Monoclinic, $P2_1/a$
a (Å)	11.415(3)	11.7247(13)	16.2904(14)
b (Å)	14.940(3)	15.0702(18)	10.7906(7)
c (Å)	10.020(2)	10.0535(10)	19.3007(18)
α (°)	97.40(3)	96.240(13)	90
β (°)	94.58(3)	95.092(13)	98.570(11)
γ (°)	109.63(3)	111.128(13)	90
V (Å^3)	1582.2(6)	1631.4(3)	3354.9(5)
Z	2	2	4
$D_{calcd.}$ (g.cm^{-1})	1.567	1.863	1.556
μ(Mo-K_α) (cm^{-1})	16.70	55.36	14.63
Data collection			
Temperature (K)	160	293	160
Diffractometer	Stoe IPDS	Stoe IPDS	Stoe IPDS
Scan mode	Φ	Φ	Φ
Scan range Φ (°)	0–250	0–250	0–250
No. of collected reflns.	15817	16326	29197
No. of unique reflns.	5882 [R(int) = 0.770]	6001 [R(int) = 0.085]	6577 [R(int) = 0.039]
No. of reflns. used	5882	6001 [$I > 2\sigma(I)$]	6577
R	0.085	0.0431	0.0267
wR_2	0.12624	0.0564	0.0634
No. of parameters	223	353	505

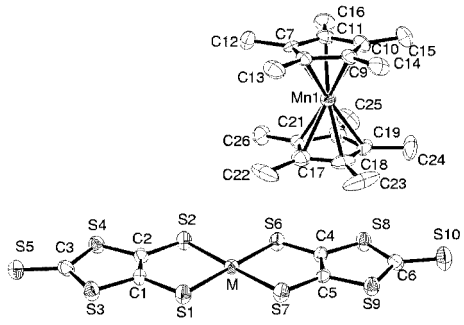

Figure 1. Atomic numbering scheme for complexes **1** and **2** (M = Ni, Au)

side $[Mn(Cp^*)_2]^+$ cations alternating with face-to-face $[M(dmit)_2]^-$ anions, the latter forming slipped dyads (Figure 2)

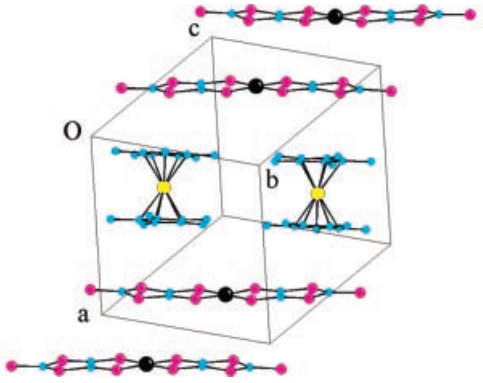

Figure 2. Structure of complexes **1** and **2** showing the ···$D^+D^+A^-A^-D^+D^+A^-A^-$··· motif

The intramolecular distances do not show any significant deviation from those observed for manganocenium-cation-based compounds[3,21] and $M(dmit)_2$-based compounds (M = Ni, Au).[11,12] The pentamethylcyclopentadienyl rings adopt approximately an eclipsed conformation, which is the opposite of the staggered conformation observed in neutral $[Mn(Cp^*)_2]$,[24] but similar to that observed in other decamethylmanganocenium-cation-containing compounds.[3,21] The planes of the Cp* rings are almost parallel to the planes of the $M(dmit)_2$ units (averaged angles of 7.84° and 5.59° for **1**; 6.27° and 4.83° for **2**) and are at averaged distances of 3.52 and 3.63 Å (for **1**) and 3.60 and 3.72 Å (for **2**).

Selected intramolecular distances and angles for **1**, **2**, $[Fe(Cp^*)_2][Ni(dmit)_2]$ and $[Fe(Cp^*)_2][Au(dmit)_2]$ are listed in Table 2. The intermolecular distances between the metal centres are very close to those found for $[Fe(Cp^*)_2]$-$[M(dmit)_2]$ (M = Ni, Au).[11,12] For an identical $M(dmit)_2$ complex, no drastic differences can be seen either between the metallic centres of a D^+D^+ pair (distance M−M in Table 2) or between the metallic centres of an A^-A^- pair (distance M′−M′ in Table 2), The largest difference (0.034 Å) occurs for the M−M′ distances, involving the metal of the cation and the metal of the anion.

Complex **3** is isostructural to $[Fe(Cp^*)_2]$-$[Ni(dmid)_2]\cdot CH_3CN$, reported in 1995 by Fettouhi and co-workers.[20] The asymmetric unit of **3** contains one molecule of acetonitrile, one $[Mn(Cp^*)_2]^+$ cation, and two halves of an $[Ni(dmit)_2]^-$ anion, each Ni atom lying on a centre of inversion (Figure 3).

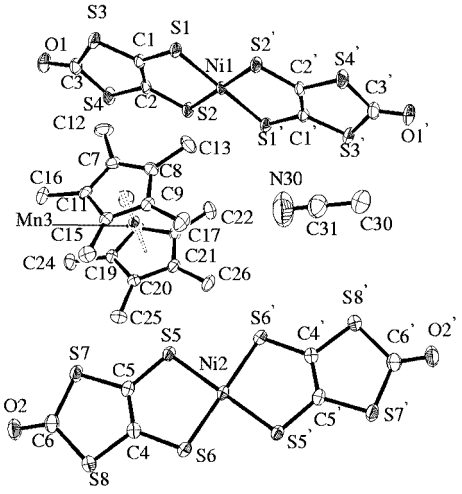

Figure 3. Atomic numbering scheme for the complex **3**

Contrary to what is observed in **1** and **2**, the overall structural arrangement of **3** consists of ···$D^+D^+A^-D^+D^+A^-$··· mixed layers parallel to the *ab* plane and separated in the *c* direction by anionic sheets of $[Ni(dmid)_2]^-$ units, which ensure neutralisation and are almost perpendicular to the mixed layers [angle of 74.35(2)° between the $Ni(dmid)_2$ units; Figure 4].

As for **1** and **2**, the planes of the Cp* rings in **3** are almost parallel to the planes of the $Ni(dmid)_2$ units in the mixed layers: they form angles of 3.38° and 3.96° and are at distances of 3.97 and 4.26 Å. Averaged and selected bond lengths and angles for **3** and $[Fe(Cp^*)_2][Ni(dmid)_2]\cdot CH_3CN$ are shown in Table 3. The Mn−Mn distance within the mixed layers is 8.250(1) Å, the shortest Mn−Ni distances are 5.911(1), 6.778(1), 6.805(1) and 7.218(1) Å and the

Table 2. Selected shortest intermolecular distances (Å) for some isostructural $[M(Cp^*)_2][M'(bis\text{-}dithiolene)_2]$ complexes

Compound	**1**	$[Fe(Cp^*)_2][Ni(dmit)_2]$	Difference	**2**	$[Fe(Cp^*)_2][Au(dmit)_2]$	Difference
M−M	8.411(8)	8.412	0.001	8.518(2)	8.523	0.005
M′−M′	5.574(8)	5.563	0.011	5.763(1)	5.755	0.008
M−M′	6.591(7)	6.557	0.034	6.564(1)	6.543	0.021
	7.330(8)	7.299	0.031	7.504(1)	7.469	0.035

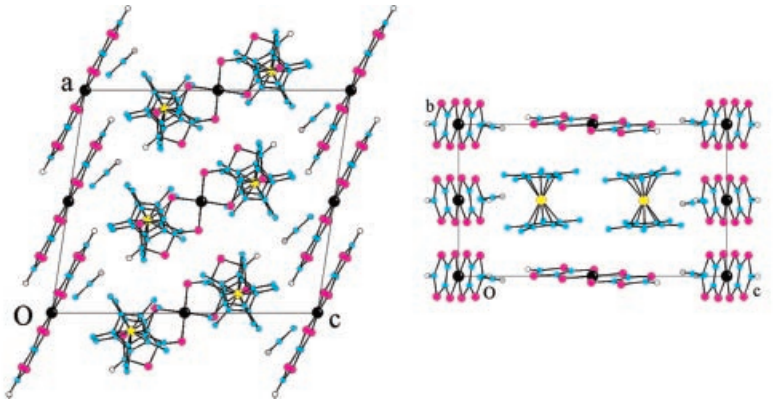

Figure 4. Projection of the structure of **3** onto the *ac* plane and onto the *bc* plane

shortest Ni−Ni distance is 9.770(1) Å. Selected intermolecular distances in **3** and in $[Fe(Cp^*)_2][Ni(dmid)_2]\cdot CH_3CN$ are also reported in Table 3. All intermolecular distances observed between metallic centres are smaller in **3** than in $[Fe(Cp^*)_2][Ni(dmid)_2]\cdot CH_3CN$, but the differences seem rather small, the largest one (0.17 Å) occurring for a large distance of ca. 11.7 Å. The Mn−S or Fe−S intermolecular distances are also similar.

Table 3. Selected shortest intermolecular distances (Å) within $[M(Cp^*)_2][Ni(dmid)_2]\cdot CH_3CN$ (M = Mn, Fe)

Compound	**3** M = Mn	$[Fe(Cp^*)_2][Ni(dmid)_2]$ M = Fe	Difference
M−M	8.250(1)	8.332(4)	0.082
Ni−Ni	9.770(1)	9.82	0.050
	11.056(1)	11.17	0.11
	11.664(1)	11.84	0.17
	13.524(1)	13.59	0.07
M−Ni	5.911(1)	6.003(2)	0.092
	6.778(1)	6.838(2)	0.060
	6.805(1)	7.268(2)	0.050
	7.218(1)		
M−S	5.426(1)	5.449(1)	0.023
	5.438(1)	5.499(6)	0.061
	5.585(1)	6.093(5)	0.010
	5.722(1)		
	6.083(1)		

Powder Diffraction

Powder diffraction was performed on sample **1** only. Analysis of the results at room temperature showed that the space group remains triclinic with the following calculated cell parameters: a = 11.5252(4) Å, b = 15.1281(5) Å, c = 10.1050(4) Å, α = 97.446(3)°, β = 94.662(3)°, γ = 109.683(3)°, to be compared with the values of 11.415(3), 14.940(3), 10.020(2) Å and 97.40(3) °, 94.58(3) °, 109.63(3)° from the single-crystal analysis at 160 K. The observed slight expansion of the lattice can be attributed to the fact that powder data were collected at room temperature, whereas the ones for single-crystal measurement were obtained at 160 K. However, the good agreement between experimental and calculated data (see Table S1 and Figure S1 in the Supporting Information) shows that the analysed powder sample retains the structure obtained from the single crystal.

Magnetic Properties of 1, 2 and 3

Magnetic studies were performed on polycrystalline powders, between 2 and 300 K.

[Mn(Cp)₂][Ni(dmit)₂] (1)*

The magnetic behaviour of **1** (in the form $\chi_M T$ versus T) is shown in Figure 5. $\chi_M T$ is equal to 1.71 emu·mol^{-1}·K at room temperature which is slightly higher than the value expected for two magnetically isolated Mn^{III} and Ni^{III} ions {1.61 emu·mol^{-1}·K, taking g values equal to 2.20 and 2.06 for $[Mn(Cp^*)_2]^+$ and $[Ni(dmit)_2]^-$, respectively}.[25,26] Such an experimental value is not surprising, since it has also been observed for several dithiolene complexes,[15,17,21,27] and is generally attributed to the anisotropic nature of the g factors of the decamethylmanganocenium[23] ion and to a partial orientation of the polycrystalline powder.

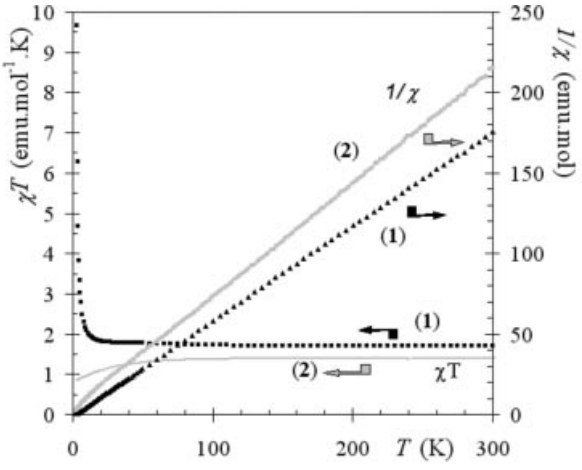

Figure 5. Temperature dependence of the magnetic susceptibility for **1** and **2**

The $\chi_M T$ value is constant down to ca. 30 K, and the plot of χ_{M-1} versus T is linear, indicating that the susceptibility of **1** follows the Curie−Weiss law, with a Weiss parameter, θ, of 2.5 K. This positive value indicates that ferromagnetic interactions dominate. As the temperature is lowered, $\chi_M T$ increases rapidly and reaches a value of 9.65 emu K mol^{-1} at 3 K. This behaviour is typical of ferromagnetic interactions. Below this temperature, the magnetic susceptibility becomes field dependent indicating that the compound exhibits a long-range magnetic ordering. This is confirmed by the field cooled (FCM), zero field cooled (ZFC) and remnant (REM) magnetisation curves shown in Figure 6a. The FCM curve presents a break around 2.5 K and the REM vanishes at the same temperature suggesting an ordering temperature, T_c, of about 2.5 K. Magnetisation versus field behaviour at 2 K is given in Figure 6b and bears out the ferromagnetic coupling between the Mn^{III} and Ni^{III} ions. At first sight, the magnetisation increases very rapidly at low field, as expected for a magnet, and then increases smoothly above 1000 G. At 50000 G, the magnetisation is equal to 2.31 μ_B, which is below the expected saturation value (3.23 μ_B), but well above the expected value for a ferrimagnetic compound (about 1.17 μ_B). Nevertheless, by carefully checking the magnetic-field dependence of **1** (see inset in Figure 6b), one can observe that the magnetisation increases sharply only up to about 1.3 μ_B. This value is already reached around 200 G, and then increases smoothly up to 2.31 μ_B at 50000 G. Such a behaviour is not consistent with the properties of a ferromagnet. Therefore **1** must be regarded as a ferrimagnet instead of a ferromagnet. Indeed, antiferromagnetic interactions between the $[Ni(dmit)_2]^-$ units ($S = 1/2$) and the $[Mn(Cp^*)_2]^+$ cations ($S = 1$) result in an $S = 1/2$ system. This is in accordance with the observed value of about 1.3 μ_B, slightly larger than 1.17 μ_B, probably due to the large anisotropy of the g factor for the $[Mn(Cp^*)_2]^+$ unit. At higher field, the antiferromagnetic interactions between the $[Ni(dmit)_2]^-$ units and the $[Mn(Cp^*)_2]^+$ cations tend to decrease, resulting in an increase of the magnetisation. Even at high field (55000 G), a slight antiferromagnetic coupling still exists between the $[Ni(dmit)_2]^-$ units and the $[Mn(Cp^*)_2]^+$ cations, which explains why saturation is not reached.

A hysteresis curve was determined at 2 K and is shown in Figure 7. The coercive field H_c is about 3.5 G and confirms that **1** is a magnet. Since these measurements were made just below T_c, this might explain the low value of H_c. Complex **1** is indeed a ferrimagnet and not a metamagnet, as confirmed by the plot of M as a function of H that does not present any curvature at low field, as was observed for $[Fe(Cp^*)_2][Ni(edt)_2]$,[19] $[Mn(Cp^*)_2][Ni(bdt)_2]$[18] and $[Mn(Cp^*)_2][M(tfd)_2]$ (M = Ni, Pd, Pt).[21]

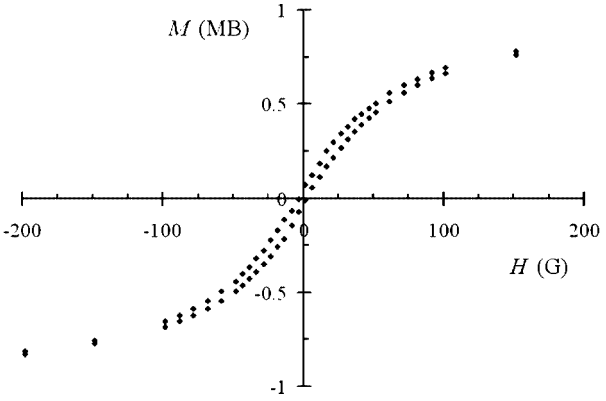

Figure 7. Hysteresis curve at 2 K for **1**

Finally, AC susceptibility measurements (Figure 8) confirm this interpretation: an out-of-phase signal is observed at 2.5 K, indicating a ferromagnetic ordering below this temperature

Such a behaviour has never been observed for any other bis-dithiolene complex. Previously studied metallocenium/metal bis-dithiolene compounds either behave as metamagnets,[18,19,21] or exhibit ferromagnetic interactions[11,15,20] but no ferromagnetic ordering has been reported. Depending on the authors, the ferromagnetic interactions in

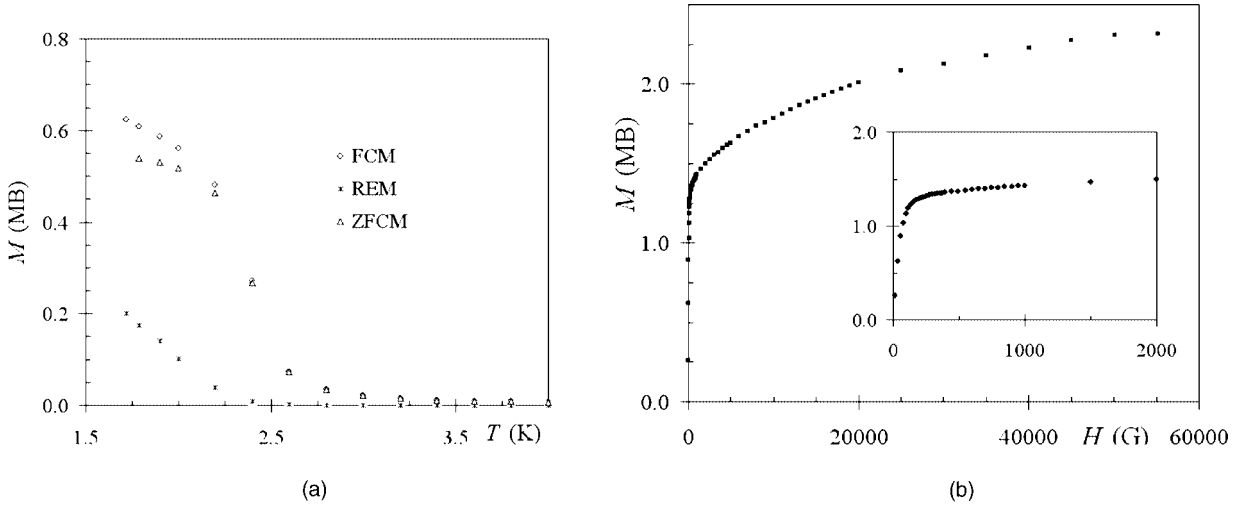

Figure 6. Temperature (a) and field dependence (b) of the magnetisation for **1**

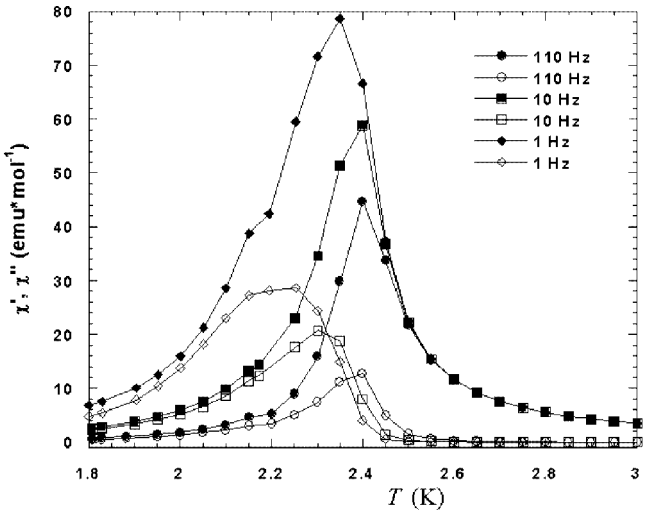

Figure 8. AC susceptibility for compound **1**

these metallocenium/metal bis-dithiolene compounds are explained by using either the McConnell mechanism II[6,11,15] (which involves charge transfer and requires the formation of $[D^{2+}]$ and $[A^{2-}]$ species) or the McConnell mechanism I[7,20] (which involves coupling between spin densities). In the latter, a global ferromagnetism arises when the interaction between spin densities of opposite sign are predominant, whereas a net antiferromagnetism results from dominant interactions between spin densities of the same sign.[28] Such a mechanism, which implies a negative spin-density located on the carbon atoms of the Cp* ring, was proposed by Kahn and co-workers[8] to explain the ferromagnetic properties in $[Fe(Cp^*)_2](TCNE)$, whereas Miller and co-workers preferred the McConnell II mechanism.[2,6] A doubt still existed as to the sign of the spin density on the carbon atoms of the Cp* ring in $[Fe(Cp^*)_2]^+$. A recent reassessment[5] of the magnetic interactions within $[Fe(Cp^*)_2](TCNE)$ has shown that a negative spin density is located on the carbon atoms of the Cp* ring, with a positive density on the carbon atoms of the methyl groups. These conclusions have been confirmed by the work of Heise and co-workers[9] on various paramagnetic metallocenium ions. Using solid-state NMR spectroscopy, these authors have shown unambiguously that a negative spin-density is located over the Cp* ring of $[Mn(Cp^*)_2]^+$ in $[Mn(Cp^*)_2](TCNE)$ and in $[Mn(Cp^*)_2](PF_6)$, and to a certain extent on the H atoms of the methyl groups, whereas a positive density on the C atoms of the methyl groups has been found, confirming previous results.[5,29] Although the stacking in **1** ($\cdots D^+D^+A^-A^-\cdots$) is different from that of $[Mn(Cp^*)_2](TCNE)$ ($\cdots D^+A^-D^+A^-\cdots$), the nature of the molecules constituting these complexes is identical: both are built from one acceptor part [TCNE or $Ni(dmit)_2$] and the same metallocenium ion. Taking these similarities and the various results into account,[5,9,29] the ferromagnetic behaviour of **1** could result from spin-polarisation effects within the McConnell I mechanism.[7] Such a mechanism is based on the interaction between the spin densities of the Cp* rings and the spin densities of the $[Ni(dmid)_2]^-$ anions.[8,30] In the $[Ni(dmit)_2]^-$ anions, positive spin-densities are observed on almost all atoms, except for the S atoms of the outer rings.[31] Three types of interaction may be considered between the spin densities of $[Mn(Cp^*)_2]^+$ and $[Ni(dmit)_2]^-$: the first interaction, between the $[Mn(Cp^*)_2]^+$ cations, should be negligible because of the large inter-cation distances ($d_{Mn-Mn} > 8.4$ Å), with the second one being between the $[Mn(Cp^*)_2]^+$ cations and the $[Ni(dmit)_2]^-$ anions and the third one between $[Ni(dmit)_2]^-$ anions within the slipped $\{[Ni(dmit)_2]_2\}^{2-}$ dyads (see Figure 2). Figure 9a clearly shows that negative-positive spin-density interactions are predominant when considering the overlap between the $[Mn(Cp^*)_2]^+$ cation and the $[Ni(dmit)_2]^-$ anion, which may result in a global ferromagnetic interaction. Within a dyad (Figure 9b), there are only two areas in which negative-positive density interactions can occur, compared to three positive-positive interactions. However, the former two zones imply the NiS_4 core, for which the spin density is larger than on the rest of the molecule, which leads to the conclusion that ferromagnetic interactions dominate also in the dyads.

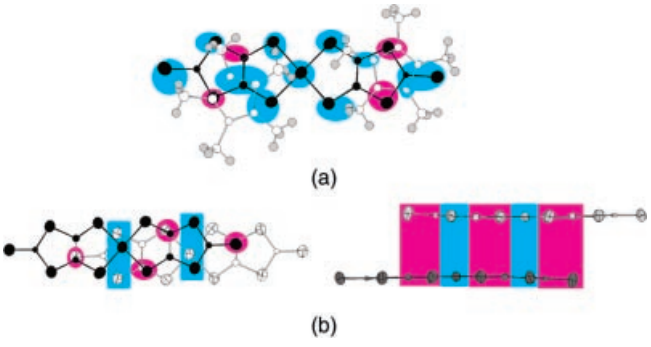

Figure 9. Modes of overlap in **1**: (a) between $[Mn(Cp^*)_2]^+$ and $[Ni(dmit)_2]^-$; (b) within a $\{[Ni(dmit)_2]_2\}^{2-}$ diad; the cyan zones represent the interactions between spin densities of opposite sign and the magenta ones represent the interactions between spin densities with the same sign

This rather qualitative approach seems to be confirmed by the preliminary results of the DFT calculations of the energy of the antiferromagnetic singlet and of the ferromagnetic triplet states as a function of the slipping within a $\{[Ni(dmit)_2]_2\}^{2-}$ dyad.[31] These calculations indicate that the minimum of energy and a ferromagnetic coupling (positive singlet-triplet gap) are observed only for slipping values close to the experimental one (3.55 Å). Consequently, the molecular arrangement in **1** could be described as favourable for ferromagnetic interactions.

$[Mn(Cp^*)_2][Au(dmit)_2]$ (2)

Magnetic measurements on **2** between 300 and 2 K lead to $\chi_M T$ values of around 1.75 emu·K·mol^{-1} at 300 K (much larger than the expected value of 1.21 emu·K·mol^{-1} calculated for an $S = 1$ isolated system, with $<g> = 2.20$). Such

a large value has already been observed in β-$[Fe(Cp^*)_2]_2$-$[Co(mnt)_2]_2$,[16] but was attributed to contamination by a small amount of ferromagnetic impurities or to traces of other metals in the starting gold complex $HAuCl_4$. If this explanation holds true in the case of **2** (in this case, the impurity might be Fe), a more reasonable value of 1.39 emu·K·mol^{-1} for the $\chi_M T$ product is reached when subtracting this ferromagnetic contribution (see Figure 5). A perfect Curie−Weiss law is then obtained, with a Weiss temperature of −4.2 K and a Curie constant of 1.42.

When lowering the temperature, the product $\chi_M T$ decreases slightly down to ca. 70 K, below which it decreases abruptly. Such a behaviour is typical of dominant antiferromagnetic interactions and is easily explained by the absence of spin carriers (Au^{III} in the $[Au(dmit)_2]^-$ units) between the pairs of manganocenium cations, which are totally isolated from each other. Therefore, no cooperative ferromagnetic interactions can occur in this complex.

[Mn(Cp)$_2$][Ni(dmid)$_2$].CH$_3$CN (3)*

The temperature dependence of $\chi_M T$ and $1/\chi_M$ for **3** is shown in Figure 10. At room temperature, the $\chi_M T$ product is 1.87 emu·K·mol^{-1}, and it increases slightly as the temperature is lowered to about 30 K. Below this temperature $\chi_M T$ increases rapidly and reaches a value of 3.66 cm^3·K·mol^{-1} at 3 K. Below 3 K, $\chi_M T$ decreases but χ_M still continues to increase. This behaviour is similar to that reported by Fettouhi and co-workers for $[Fe(Cp^*)_2]$-$[Ni(dmid)_2]$·CH_3CN.[20] and is typical of dominant ferromagnetic interactions to which weak antiferromagnetic interactions are superimposed. The plot of χ_{M-1} versus T is linear, indicating that the susceptibility of **3** follows the Curie−Weiss law, with a Weiss temperature, θ, of 2.80 K, larger than the one obtained for $[Fe(Cp^*)_2]$-$[Ni(dmid)_2]$·CH_3CN.

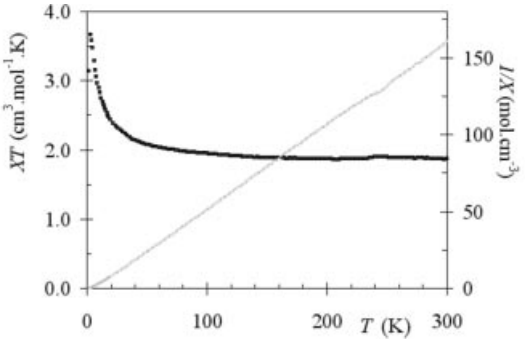

Figure 10. Temperature dependence of the magnetic susceptibility for **3**

The similarity in the behaviours of **3** and $[Fe(Cp^*)_2]$-$[Ni(dmid)_2]$·CH_3CN is not totally surprising as it is only the nature of the metal that changes in the decamethylmetallocenium ion. In contrast, we did not expect that substituting an oxygen atom for a sulfur atom when going from the $Ni(dmit)_2$ complex (**1**) to the $Ni(dmid)_2$ complex (**3**) could lead to such different structural arrangements, and consequently to very different magnetic properties. A possible explanation for the magnetic properties of **3** could be similar to that proposed by Fettouhi and co-workers in the case of $[Fe(Cp^*)_2][Ni(dmid)_2]$·CH_3CN,[20] which is based on the interaction between the negative spin-density of the Cp* rings and the positive spin-density of the sulfur atoms of the $[Ni(dmid)_2]^-$ anions.[30] Indeed, as shown in Figure 11, the overlap between $[Mn(Cp^*)_2]^+$ and $[Ni(dmid)_2]^-$ is such that interactions between spin densities of opposite sign are largely predominant. Unfortunately, however, in the case of **3** there is no clear-cut experimental evidence supporting this interpretation, as was the case for **1**.

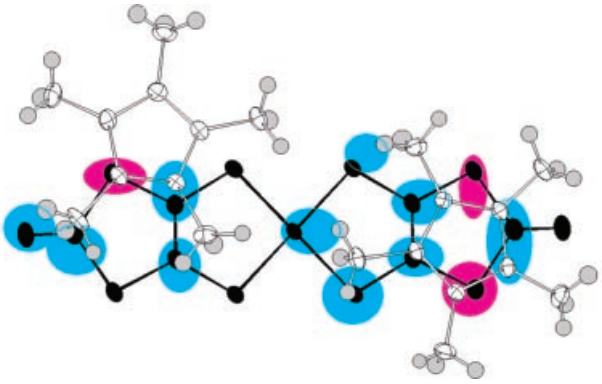

Figure 11. Modes of overlap in **3** between $[Mn(Cp^*)_2]^+$ and $[Ni(dmid)_2]^-$ in the mixed layer; the cyan zones represent the interactions between spin densities of opposite sign and the magenta ones the interactions between spin densities with the same sign

Conclusion

We have shown that by using the same cation $[Mn(Cp^*)_2]^+$ with two different 1,2-bisdithiolene metal complexes $[Ni(dmit)_2$ and $Ni(dmid)_2]$, drastic changes in the structural arrangements occur. This leads to various magnetic properties, with different behaviour. The present study has allowed us to reiterate that in compounds based on metal bis-dithiolene complexes $[M(S_2C_2R_2)_2]^-$ a $D^+A^-D^+A^-$ motif in the structural arrangement is not a prerequisite for promoting ferromagnetic interactions, let alone ferromagnetism. The selection of the $[Mn(Cp^*)_2]^+$ cation, as already recommended by Broderick et al.,[21] has led to compounds which exhibit even more interesting properties than the $[Fe(Cp^*)_2]^+$-based compounds. For example, **1** is the first ferrimagnet to be derived from a metal bis-dithiolene complex whereas $[Fe(Cp^*)_2][Ni(dmit)_2]$ exhibits only ferromagnetic interactions, and **3** presents stronger ferromagnetic interactions than its iron analogue, $[Fe(Cp^*)_2][Ni(dmid)_2]$·CH_3CN. Nevertheless, due to the complexity and diversity of the structures, and in spite of possible comparison with various compounds, the understanding of their magnetic behaviour remains at the qualitative level. Theoretical DFT calculations are currently in progress to give a better insight into

the origin of the ferromagnetism in **1**.[31] Solid-state NMR spectroscopy, as shown by Heise and co-workers,[9] should provide qualitative as well as quantitative information on the interactions within these materials. Such a study seems to be a very promising tool, since it will take both the intra- and intermolecular effects into account. Indeed, the determination of structure-magnetism relationships in molecular magnetic materials requires not only the study of the direct overlap between neighbouring molecules, but also the consideration of the global packing of the structure, as shown by Veciana and co-workers for α-nitronyl nitroxide radicals.[32] It is important to note that only short intermolecular effects have been considered for the qualitative interpretation of the results reported here. Several complexes based on the $[Mn(Cp^*)_2]^+$ cation and metal complexes of the $dmid^{2-}$ ligand are being studied at present, in order to expand the range of compounds exhibiting such ferromagnetic interactions without the $D^+A^-D^+A^-$ motif.[33]

Experimental Section

General Remarks: Bis(pentamethylcyclopentadienyl)manganese(III) hexafluorophosphate $[Mn(Cp^*)_2]PF_6$ was synthesised from pentamethylferrocenium hexafluorophosphate $[FeCp_2]PF_6$ following the procedure reported by Robbins and co-workers.[23] Tetrabutylammonium bis(1,3-dithiol-2-thione-4,5-dithiolato)nickelate(III), $(nBu_4N)[Ni(dmit)_2]$, tetrabutylammonium bis(1,3-dithiol-2-thione-4,5-dithiolato)aurate(III), $(nBu_4N)[Au(dmit)_2]$, and tetraphenylarsonium bis(1,3-dithiol-2-one-4,5-dithiolato)nickelate(III), $(AsPh_4)[Ni(dmid)_2]$, were synthesised following the literature procedures.[26,34,35] All solvents were dried and distilled prior to use. All syntheses were carried out in an inert atmosphere box or using Schlenk techniques.

$[Mn(Cp^*)_2][Ni(dmit)_2]$ (1): This compound was obtained after slow addition of an acetonitrile solution of $[Mn(Cp^*)_2]PF_6$ (194 mg, 0.413 mmol) to an acetonitrile solution of $(nBu_4N)[Ni(dmit)_2]$ (265 mg, 0.382 mmol). Partial removal of the solvent under reduced pressure, followed by filtration, afforded a brown microcrystalline powder, which was washed several times with acetonitrile and dried in vacuo. $C_{26}H_{30}MnNiS_{10}$ (776.75): calcd. C 40.20, H 3.89, S 41.27; found C 39.62, H 3.26, S 41.15.

$[Mn(Cp^*)_2][Au(dmit)_2]$ (2): Compound **2** was synthesised following the same procedure as for **1**, using 26 mg (0.031 mmol) of $(nBu_4N)[Au(dmit)_2]$, dissolved in 15 mL of acetone and 18 mg (0.038 mmol) of $[Mn(Cp^*)_2]PF_6$ dissolved in 10 mL of acetonitrile. $C_{26}H_{30}AuMnS_{10}$ (915.01) (**2**): calcd. C 34.12, H 3.31, S 35.04; found C, 34.02, H 3.30, S 34.97.

$[Mn(Cp^*)_2][Ni(dmid)_2]\cdot CH_3CN$ (3): Compound **3** was synthesised following the same procedure as for **1**, using 196 mg (0.244 mmol) of $(AsPh_4)[Ni(dmid)_2]$ dissolved in 30 mL of acetonitrile and 122 mg (0.259 mmol) of $[Mn(Cp^*)_2]PF_6$ dissolved in 25 mL of acetonitrile. $C_{28}H_{33}MnNNiO_2S_8$ (785.68): calcd. C 42.80, H 4.24, S 32.64; found C, 42.52, H 4.16, S 31.85.

Magnetic Measurements: DC magnetic data were recorded on a MPMS5 magnetometer (Quantum Design Inc.). The calibration was made at 298 K using a palladium reference sample furnished by Quantum design Inc. AC susceptibility was measured on a SQUID magnetometer Quantum Design MPMS-XL-5.

X-ray Crystallographic Study: The experimental details and crystal data are listed in Table 1. Data collection and cell refinement were performed with a sealed Mo-K_α (λ = 0.71073 Å) X-ray source on a Stoe Imaging Plate Diffraction System (IPDS) diffractometer, using the IPDS software.[36] Crystal decay was monitored by measuring a maximum of 200 reflections per image. The structures were solved using Sir97[37] or Shelxs97[38] and refined with Shelxl97.[39] The calculations were carried out with the WinGX package program[40] running on a PC. The drawings of the molecular structures were performed with CAMERON,[41] ORTEP.[42] The atomic scattering factors are taken from the International Tables for X-ray Crystallography.[43]

$[Mn(Cp^*)_2][Ni(dmit)_2]$ (1): A brown rhombic plate (0.1 mm side and 0.02 mm thick) was selected for the X-ray study. The crystal-to-detector distance was 70 mm. 133 exposures (6 min per exposure) were obtained with $0 < \Phi < 250°$ and with the crystals rotated through 1.5° in Φ in the oscillation mode.

$[Mn(Cp^*)_2][Au(dmit)_2]$ (2): A brown elongated bar ($0.37 \times 0.05 \times 0.05$ mm^3) was selected for the X-ray study. The crystal-to-detector distance was 70 mm. 167 exposures (5 min per exposure) were obtained with $0 < \Phi < 250°$ and with the crystals rotated through 1.5° in Φ in the oscillation mode.

$[Mn(Cp^*)_2][Ni(dmid)_2]\cdot CH_3CN$ (3): A black squared-shaped thick plate (0.23 mm side and 0.1 mm thick) was selected for the X-ray study. The crystal-to-detector distance was 70 mm. 209 exposures (3 min per exposure) were obtained with $0 < \Phi < 250°$ and with the crystals rotated through 1.2° in Φ in the oscillation mode.

Full details related to every compound are given in the Supporting Information.

CCDC-203647 (**1**), -203646 (**2**) and -203645 (**3**) contain the supplementary crystallographic data for this paper. These data can be obtained free of charge at www.ccdc.cam.ac.uk/conts/retrieving.html [or from the Cambridge Crystallographic Data Centre, 12, Union Road, Cambridge CB2 1EZ, UK; Fax: (internat.) +44-1223/336-033; E-mail: deposit@ccdc.cam.ac.uk].

X-ray Powder Diffraction Studies

The sample was prepared in a side-filling cell, in order to minimise preferred orientations. The data were collected with a Seifert XRD 3000 TT diffractometer in Bragg−Brentano (Θ − Θ) configuration, using Cu-K_α radiation, fitted with a graphite diffracted-beam monochromator, in the interval $2° < \Theta < 30°$. The raw data were treated with the PowderX program,[44] in order to recalculate the cell parameters, and compared to the simulated diagram obtained with CaRine.[45]

Supporting Information [Table S1 (Miller indices and experimental and calculated $1/d^2hkl$ with the relative intensity of the experimental value], Figure S1 [experimental and calculated X-ray powder diagram for compound **1**, and the cif files for **1**, **2** and **3**] is available. See footnote on the first page of this article.

Acknowledgments

The support and sponsorship provided by COST Action D14/0003/99 are acknowledged. We are also deeply indebted to J. Cano and Y. Journaux for communicating the preliminary results of their DFT calculations and for enlightening discussions. Technical assistance by A. Mari for magnetic measurements is gratefully acknowledged. The authors are also grateful to Dr. Cheng Dong (National Labor-

atory for Superconductivity, Institute of Physics, Chinese Academy of Science, Beijing) for free licensing his program PowderX.

[1] G. A. Candela, L. Swartzendruber, J. S. Miller, M. J. Rice, *J. Am. Chem. Soc.* **1979**, *101*, 2755−2756.
[2] J. S. Miller, J. C. Calabrese, H. Rommelmann, S. R. Chittipeddi, J. H. Zhang, W. M. Reiff, A. J. Epstein, *J. Am. Chem. Soc.* **1987**, *109*, 769−781.
[3] W. E. Broderick, J. A. Thompson, E. P. Day, B. M. Hoffman, *Science* **1990**, *249*, 401−403.
[4] G. T. Yee, J. M. Manriquez, D. A. Dixon, R. S. McLean, D. M. Groski, R. B. Flippen, K. S. Narayan, A. J. Epstein, J. S. Miller, *Adv. Mater.* **1991**, *3*, 309−311.
[5] J. Schweizer, A. Bencini, C. Carbonera, A. J. Epstein, S. Golhen, E. Lelièvre-Berna, J. S. Miller, L. Ouahab, Y. Pontillon, E. Ressouche, A. Zheludev, *Polyhedron* **2001**, *20*, 1771−1778.
[6] H. M. McConnell, *Proc. Robert A. Welch Found. Conf. Chem. Res.* **1967**, *11*, 144−145.
[7] H. M. McConnell, *J. Chem. Phys.* **1963**, *39*, 1910.
[8] C. Kollmar, M. Couty, O. Kahn, *J. Am. Chem. Soc.* **1991**, *113*, 7994−8005.
[9] H. Heise, F. H. Köhler, M. Herker, W. Hiller, *J. Am. Chem. Soc.* **2002**, *124*, 10823−10832.
[10] J. S. Miller, A. J. Epstein in *Research Frontiers in Magnetochemistry* (Ed.: C. J. O'Connor), World Scientific Publisher, Singapore, **1993**, pp 283−302.
[11] W. E. Broderick, J. A. Thompson, M. R. Godfrey, M. Sabat, B. M. Hoffman, E. P. Day, *J. Am. Chem. Soc.* **1989**, *111*, 7656−7657.
[12] G. Matsubayashi, A. Yokozawa, *Inorg. Chim. Acta* **1992**, *193*, 137−141.
[13] S. Tanaka, G. Matsubayashi, *J. Chem. Soc., Dalton Trans.* **1992**, 2837−2843.
[14] S. Rabaca, V. Gama, D. Belo, I. C. Santos, M. T. Duarte, *Synth. Met.* **1999**, *103*, 2302−2303.
[15] J. S. Miller, J. C. Calabrese, A. J. Epstein, *Inorg. Chem.* **1989**, *28*, 4230−4238.
[16] M. Fettouhi, L. Ouahab, M. Hagiwara, E. Codjovi, O. Kahn, H. Constant-Machado, F. Varret, *Inorg. Chem.* **1995**, *34*, 4152−4159.
[17] W. B. Heuer, P. Mountford, M. L. H. Green, S. G. Bott, D. O′Hare, J. S. Miller, *Chem. Mater.* **1990**, *2*, 764−772.
[18] V. Gama, D. Belo, I. C. Santos, R. T. Henriques, *Mol. Cryst. Liq. Cryst.* **1997**, *306*, 17−24.
[19] V. Gama, D. Belo, S. Rabaça, I. C. Santos, H. Alves, J. C. Waerenborgh, M. T. Duarte, R. T. Henriques, *Eur. J. Inorg. Chem.* **2000**, 2101−2110.
[20] M. Fettouhi, L. Ouahab, E. Codjovi, O. Kahn, *Mol. Cryst., Liq. Cryst.* **1995**, *273*, 29−33.
[21] W. E. Broderick, J. A. Thompson, B. M. Hoffman, *Inorg. Chem.* **1991**, *30*, 2958−2960.
[22] C. Faulmann, A. E. Pullen, E. Riviere, Y. Journaux, L. Retailleau, P. Cassoux, *Synth. Met.* **1999**, *103*, 2296−2297.
[23] J. L. Robbins, N. M. Edelstein, S. R. Cooper, J. C. Smart, *J. Am. Chem. Soc.* **1979**, *101*, 3853−3857.
[24] D. P. Freyberg, J. L. Robbins, K. N. Raymond, J. C. Smart, *J. Am. Chem. Soc.* **1979**, *101*, 892−897.
[25] J. S. Miller, R. S. McLean, C. Vazquez, G. T. Yee, K. S. Narayan, A. J. Epstein, *J. Mater. Chem.* **1991**, *1*, 479−480.
[26] R. Kirmse, J. Stach, W. Dietzsch, G. Steimecke, E. Hoyer, *Inorg. Chem.* **1980**, *19*, 2679−2685.
[27] V. Gama, S. Rabaca, C. Ramos, D. Belo, I. C. Santos, M. T. Duarte, *Mol. Cryst. and Liq. Cryst.* **1999**, *335*, 81−90.
[28] For a nice illustration based on the allyl radical, see: O. Kahn, *Molecular Magnetism* Wiley VCH, New York, **1993**, 303−309.
[29] J. Blümel, N. Hebendanz, P. Hudeczek, F. H. Köhler, W. Strauss, *J. Am. Chem. Soc.* **1992**, *114*, 4223−4230.
[30] C. Kollmar, O. Kahn, *Acc. Chem. Res.* **1993**, *26*, 259−265.
[31] Y. Journaux, J. Cano, personal communication.
[32] M. Deumal, J. Cirujeda, J. Veciana, J. J. Novoa, *Chem. Eur. J.* **1999**, *5*, 1631−1642.
[33] C. Faulmann, E. Rivière, S. Dorbes, P. Cassoux, *manuscript in preparation*.
[34] G. Steimecke, H. J. Sieler, R. Kirmse, E. Hoyer, *Phosphorus Sulfur* **1979**, *7*, 49−55.
[35] R. Vicente, J. Ribas, C. Faulmann, J. P. Legros, P. Cassoux, *C. R. Acad. Sci., Ser. II* **1987**, *305*, 1055−1058.
[36] Stoe, *IPDS Software, version 2.86*, Darmstadt, Germany, 1996.
[37] A. Altomare, M. C. Burla, M. Camalli, G. L. Cascarano, C. Giacovazzo, A. Guagliardi, A. G. G. Moliterni, G. Polidori, R. Spagna, *J. Appl. Cryst.* **1999**, *32*, 115−119.
[38] G. M. Sheldrick *SHELXS-97- A Program for Automatic Solution of Crystal Structure (Release 97−2):* Institüt für Anorganische Chemie der Universität, Tammanstrasse 4, 3400 Göttingen, Germany, **1997**.
[39] G. M. Sheldrick *SHELXL-97- Programs for Crystal Structure Analysis (Release 97−2):* Institüt für Anorganische Chemie der Universität, Tammanstrasse 4, 3400 Göttingen, Germany, **1998**.
[40] L. J. Farrugia, *J. Appl. Cryst.* **1999**, *32*, 837−838.
[41] D. M. Watkin, L. Pearce, C. K. Prout *CAMERON − A Molecular Graphics Package:* Chemical Crystallography Laboratory, University of Oxford, **1993**.
[42] L. J. Farrugia *J. Appl. Crystallogr.,* 1997; Vol. 30, pp 565.
[43] *International Tables for Crystallography, Volume A* (Ed.: T. Hahn), Kluwer Academic Publishers: Dordrecht, The Netherlands, **1995**.
[44] C. Dong *PowderX:* Institute of Physics, Beijing.
[45] ESM *CaRine Crystallography*; v; 3.1 ed.; ESM Software: Hamilton, OH 45013, USA.

Received February 13, 2003

